Experimental Study on Relative Flow Regime and Broadband Noise of a Propeller Fan

Soichi Sasaki, Hisanari Hidaka

Experimental Study on Relative Flow Regime and Broadband Noise of a Propeller Fan

Soichi Sasaki[1]*, Hisanari Hidaka[2]

ISROMAC 2017

International Symposium on Transport Phenomena and Dynamics of Rotating Machinery

Hawaii, Maui

December 16-21 2017

Abstract

The aim of this study is to clarify the relationship between the broadband noise from the low frequency to transition frequency domain generated from the propeller fan and the relative flow regime. In the off design operation condition, the velocity fluctuation having a lower frequency than the blade passing frequency was formed at the leading edge of the blade tip side. The low frequency broadband noise in the off design operation condition has feasibility to generate at the leading edge by adjoined blade interference of the lower frequency than the blade passing frequency. The major factor of the fan noise in the design operation condition was the broadband noise in the transition frequency. From the analysis of CFD, we clarified when the unstable wave due to Karman vortex shedding resonates with the air column resonance frequency made by the blade passage, the pressure fluctuation having a specific frequency is enhanced. These results indicated that the noise in the specific frequency band increased, even though the fan is operated in the design flow rate, when the air column resonance in the blade passage was superimposed to the span direction.

Keywords

Aeroacoustics, Broadband Noise, Propeller, Fan,

[1] *Division of System Science, Graduate School of Engineering, Nagasaki University, Japan*
[2] *Department of Advanced Engineering, Graduate School of Engineering, Nagasaki University, Japan*
***Corresponding author**: souichi@nagasaki-u.ac.jp

INTRODUCTION

Propeller fans are widely used in a heat exhaust fan, a ventilation fan, and an engine cooling fan, and so on. Therefore, the improvement not only to increase the aerodynamic performance but also to decrease the fan noise is one of the important technical issues. For example, the fan used for the engine cooling is driven at the off-design point in the low flow rate condition because of the resistance of the engine block [(1)]. The cooling fan used in the outdoor unit of an air conditioner is also driven in the low flow rate domain due to the resistance of the heat exchanger or the griller [(2)]. Thus, the noise characteristics of the fan under the driving condition in the low flow rate domain, that is, fan noise in the off design operation condition have been discussed in the preceding studies.

In 2001, Jang, C.-M. et al investigated three-dimensional structures of the vortical flow field in a propeller fan by experimental analysis using laser doppler velocimetry measurements [(3-4)]. According to the results of their investigation, the tip vortex formed near the mid chord of the blade tip suction surface convects almost in the tangential direction, thus impinging on the pressure surface of the adjacent blade. In 2004, T. Fukano et al studied that the noise due to tip clearance flow in the axial flow fans operating at the design and off-design conditions is analyzed by an experimental measurement [(5)]. They clarified that the fan noise increased due to tip clearance flow at low flow rate condition. They also indicated that the noise was generated due to the interference on the tip leakage vortex and the pressure surface of the adjoined blade. On the other hand, since the axial fan in the design operation condition flows to the axial direction, the relative flow becomes hard to interfere with the adjacent blade. In this case, except for the discrete frequency noise generated due to mechanical irregularity of the blade row [(6)], the broadband noise becomes the important factor of the aerodynamic noise generated from the fan. Fukano, et al have also proposed a prediction theory in which the broadband noise generated by the Karman vortex shedding based on the experiment of a rotating isolated blade [(7)]. In the prediction theory, the broadband noise of the predicted value in the lower frequency domain than the center frequency of the vortex shedding became small than the measured value, but the mechanism cause is not mentioned. In 2005, for the establishment of the analytical model of the broadband noise, M. Roger and S. Moreau [(8)] have been suggested the analytical model further extensions of the Amiet's trailing edge model [(9)]. However, the analytical model is for the broadband noise in the relatively high frequency domain, that is, this analytical model is distinguished from the broadband noise in the low frequency domain.

The aim of this study is to clarify the relationship between the broadband noise in the low frequency domain generated from the propeller fan and the relative flow field. First of all, the aerodynamic characteristics and noise of the actual propeller fan are measured; the relative flow field of the blade tip at the design operation condition and the off design operation condition is measured by the phase lock method of hot-

wire anemometer. In order to analyze the pressure fluctuation in the blade passage by the small calculation capacity, the relative flow field in the blade passage is analyzed by the two-dimensional blade cascade model of the annular cylinder. Based on the analysis of the relative flow field by the measurement and CFD, we discuss the mechanism of the broadband noise distributed within the low frequency to transition frequency.

NOMENCLATURE

c : Blade chord	[mm]
D : Diameter of the impeller	[mm]
f : Frequency	[Hz]
L : shaft power	[kW]
L_A : Noise level	[dB]
N : Rotation speed	[rpm]
Q : Flow rate	[m^3/s]
p : pressure	[Pa]
p_0 : base sound pressure（20μPa）	[Pa]
R : Radius of the impeller	[mm]
r : Location in the span direction	[mm]
U : circumferential velocity	[m/s]
V : absolute velocity	[m/s]
W : relative velocity	[m/s]
Z : number of blades	
ρ : density	[kg / m^3]
ξ : mainstream direction	[mm]
η : efficiency	
η_θ : circumferential direction	[mm]
v : hub tip ratio	
θ : deviation angle	[°]
φ : flow rate coefficient	
ψ_s : static pressure coefficient	
‘ : velocity fluctuation	
¯ : time mean velocity	

1. EXPERIMENTL SETUP

Figure 1 is the schematic diagram of the test bench for the estimation of the fan performance. The diameter of the impeller is 613 mm, the hub ratio is 0.424 and number of blades is 14. The measurement method for the aerodynamic performance of the fan is shown in Fig. 1 (a). The height and width of the duct are 1 m each, while its total length is approximately 4 m. The dynamic pressure is measured 600 mm upstream of the impeller disc using a Pitot tube. From the results of the velocity distribution for the estimation of the flow rate, the flow coefficient was found to be 0.842. The flow rate is deduced from the dynamic pressure. It is controlled by an adjustable throttle at the duct exit. The static pressure of the fan is measured 400 mm upstream of the exit. The rotational speed of the driving shaft is 1200 rpm. We measured the shaft torque of the motor using a torque meter (Ono-Sokki; SS-500), and the efficiency of the fan was estimated based on the ratio of shaft power to theoretical power. The normalized characteristics of the fan are summarized as follows.

$$\phi = \frac{4\,Q}{\pi\,(1-\nu^2)\,D^2\,U},\ \psi_s = \frac{2P_s}{\rho\,U^2}$$
$$\lambda = \frac{8\,L}{\rho\,\pi\,(1-\nu^2)\,D^2\,U^3},\ \eta = \frac{\varphi\,\psi_s}{\lambda} \quad (1)$$

where the φ is the flow coefficient, ψ_s is the static pressure coefficient, λ is the power coefficient, and η is the efficiency. The experimental setup for the fan noise measurement is shown in Fig. 1 (b). A 1/2-inch microphone (Ono-Sokki, LA-4350) is set at distance of 1.0 m from the impeller inlet on the rotational axis of the impeller. The frequency signal of the measured fan noise is provided by a Fast Fourier Transfer analyzer (Ono Sokki, CF5210).

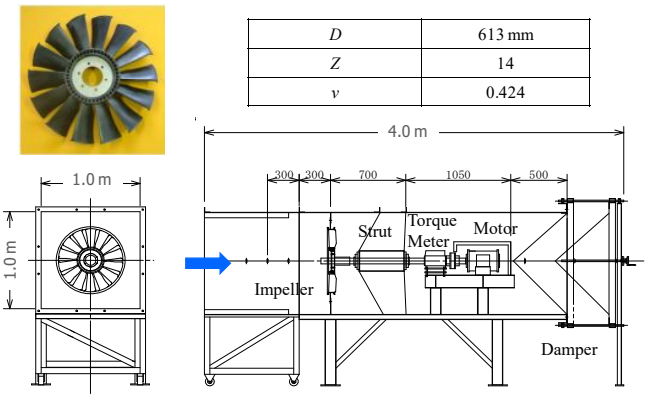

(a) Aerodynamic performance

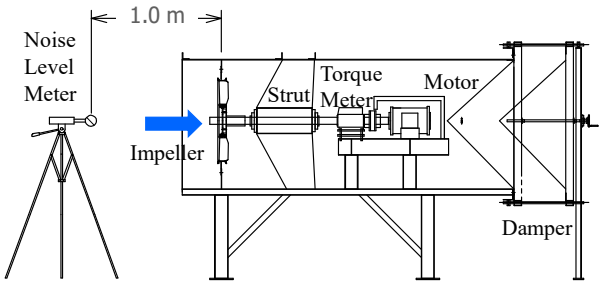

(b) Fan noise

Fig. 1 Schematic diagram of the test bench for the estimation of the fan performance

In Fig. 2, the measurement method of the flow field in the blade tip is shown. The internal flow of the fan is measured by an X type hot-wire probe (KANOMAX, 0249R-T5). The X type hot wire probe can be possible to simultaneously measure the two velocity components. The hot-wire probe is attached to the traverse machine; the arbitrary flow field is measured by controlling the stepping motor. The domain of the upstream and downstream is divided by a steel partition (SS400, 3.2 mm). The clearance between the partition and the blade

tip is 7 mm. The flow regime near the blade tip is measured 160 mm in the mainstream directions and 240 mm in the radial directions. The measurement position of the wake is 5 mm behind the trailing edge of the blade. The time mean velocity of the absolute velocity and the relative velocity is expressed by the equation (2).

$$v = \overline{v} + v' \,,\; w = \overline{w} + w' \qquad (2)$$

where, v is the absolute velocity, w is the relative velocity, $\overline{\ }$ is the time mean, and $'$ is the fluctuation component. As shown in the velocity triangle, when the circumferential velocity of the impeller rotates at a constant velocity, the fluctuation variation of the absolute velocity and the relative velocity becomes same.

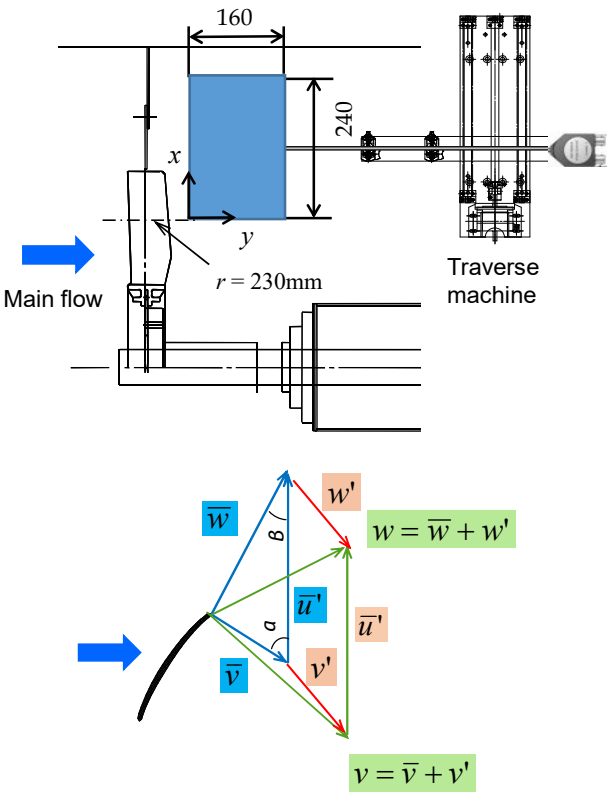

Fig. 2 measurement method of the flow field in the blade tip

The measurement method by the phase-lock method in the relative flow field of the blade tip is shown in Fig. 3. In order to measure the relative flow field in the blade tip, the flow field from -12 mm to 80 mm is measured with 4 mm interval as the base criterion of the leading edge. The three velocity components is measured by the X type hot-wire probe rotated 90 degrees. The signal synchronized with the main shaft is picked up by the photonics rotational detector (Ono-Sokki, MP-911). Then, the signal is input to the FFT analyzer as the trigger signal. The phase of the variable signal of the blade tip is locked by using a trigger signal synchronized with the rotation of the rotor axis to analyze the structure of a time-mean flow of the blade passage. At this time, when the circumferential velocity of the blade tip is multiplied to the time variable signal, the spatial relative flow can be measured from the absolute flow coordinate.

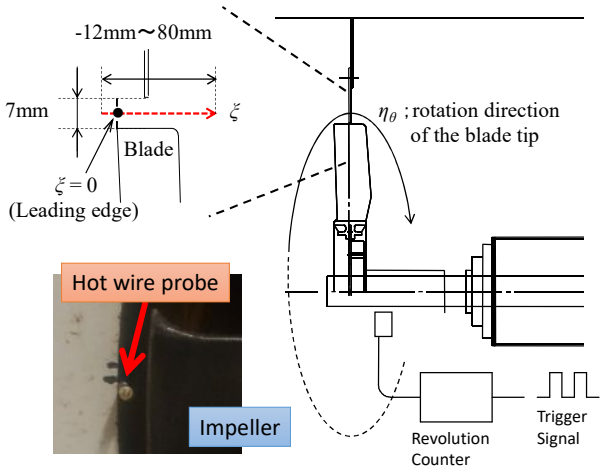

Fig. 3 Measurement method by the phase-lock method in the relative flow field of the blade tip

In Fig. 4, the CFD model of a two-dimensional blade cascade of the propeller fan is shown. In this study, the two dimensional blade cascades is created in the annular cylinder with the 4 mm thickness, in which the aim of suppressing the calculation load and analyzing the pressure fluctuation of the blade cascade with high resolution. Main flow velocity estimated by the design flow rate is given to the inlet boundary and the atmospheric pressure is given to the exit side boundary. The minimum grid width is set so that y^+ <10 (approximately 70 μm). The number of elements of this model is approximately 3.9 million. Cradle SCRYU Tetra V13 is used for the solver. From the quasi-steady state, 2048 cycles are iteratively calculated. The time interval is given so that the Courant number is about 1.0. The rotation speed of the blade row is 1200 rpm. In order to obtain the unsteady pressure on the blade surface, 26 measurement points are set on the blade surface.

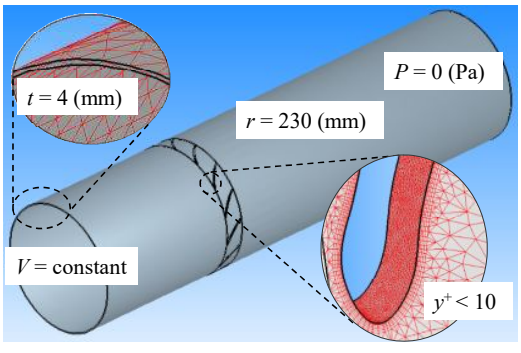

Fig. 4 CFD model of a two-dimensional blade cascade of the propeller fan

2. RESULTS AND DISCUSSION

2.1 Broadband noise of off design

The aerodynamic characteristics of the fan in the different rotational speed are compared in Fig. 5. The aerodynamic characteristic becomes the similarity property at a rotation speed of 1000 rpm or more. The maximum efficiency point is in the vicinity of φ = 0.3. In the following analysis, the flow rate coefficient 0.3 is employed as the design point, whereas the flow rate coefficient 0.17 is defined as the off design point. In Fig. 6, the characteristics of the fan noise are shown. On the design point, when the rotation speed becomes high, the noise level becomes large. However, the difference of the noise level to the flow rate in each rotation speed is little around the design point. On the other hand, the noise level is increased when the flow rate is decreased to the off design point.

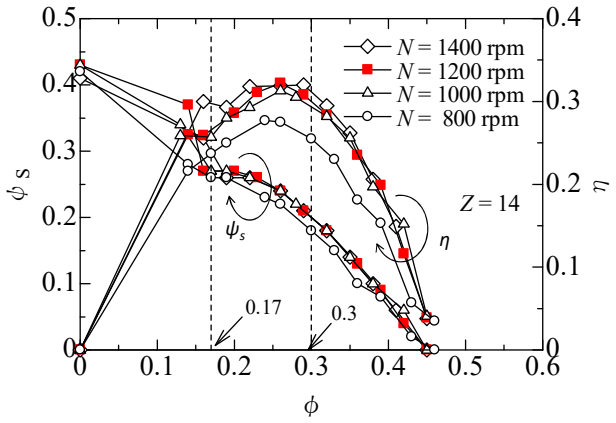

Fig. 5 Aerodynamic characteristics of the fan in the different rotational speed

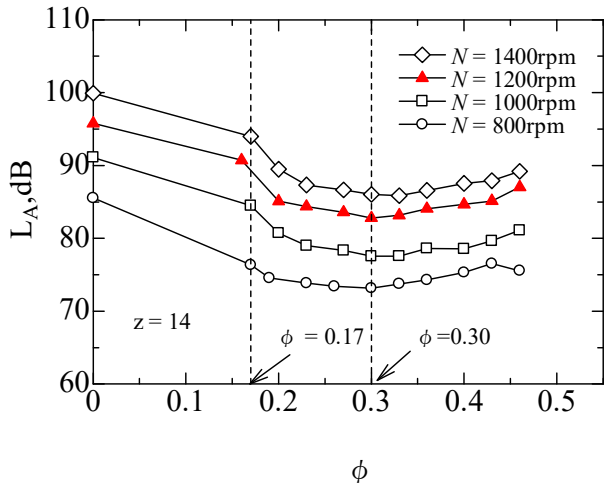

Fig. 6 Characteristics of the fan noise

In Fig. 7, the spectral distributions of the fan noise on the design flow rate and the off design flow rate are compared. In the following analysis, for convenience, the frequency band below 500 Hz is referred to as low frequency, the band from 500 Hz to 2000 Hz as transition frequency, and the band above 2000 Hz as high frequency. The broadband noise at the off design operation condition becomes large than the design operation condition due to adjoined blade interference of the tip vortex [5]. It is considered that the broadband noise in the high frequency domain is caused by trailing edge noise [9]. The discrete frequency noise (DFN) synchronized with the blade passing frequency (BPF = 280 Hz) is generated from the fan at the design operation condition. It has feasibility that the discrete frequency noise is due to the mechanical irregularity of the impeller [6]. The dominant factor of the fan noise in the design flow rate is the broadband noise in the low frequency to the transition frequency except for the discrete frequency noise. The broadband noise in the transition frequency is larger than the high frequency broadband noise, moreover, the property of the frequency distribution is different from the trailing edge noise in the high frequency.

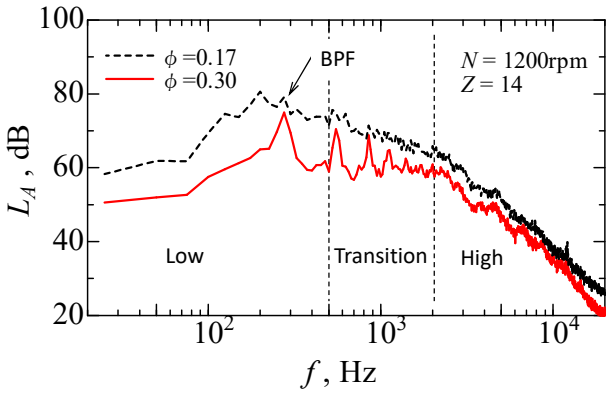

Fig. 7 Spectral distributions of the fan noise on the design flow rate and the off design flow rate

The distributions of the axial velocity component of the absolute velocity in the meridian plane are shown in Fig. 8. The broken line in the figure is the position of the blade tip. The wake flow in the design operation condition flows to the axial direction (see Fig. 8 (a)). In the case of the off design flow rate, the flow regime is expanded to the radial direction like a centrifugal fan due to the back pressure (see Fig. 8 (b)). This flow regime implies that the flow around the impeller at the off design operation condition becomes the swirl flow.

In Fig. 9, the distributions of the absolute velocity in the relative flow field at the blade tip are shown. The main flow flows from top to bottom toward the paper surface; the impeller rotates from right to left. The upper figure is the velocity distribution of the design flow rate, and the lower one is that of the off design flow rate. In the both operating condition, since the direction of the flow on the suction surface at the leading edge is deflected by the blade, the circumferential velocity on the suction surface at the leading is increased. The axial flow velocity in the vicinity of the leading edge in the off design flow rate becomes small, and its relative flow swirls to the circumferential direction. Furthermore, the wake near the trailing edge of the off design flow rate

flows to the circumferential direction more than that of the design point. There is also a flow field having a small axial velocity in the vicinity of the leading edge of the design flow rate, and then the relative flow in the domain also becomes the weak swirling flow to the circumferential direction.

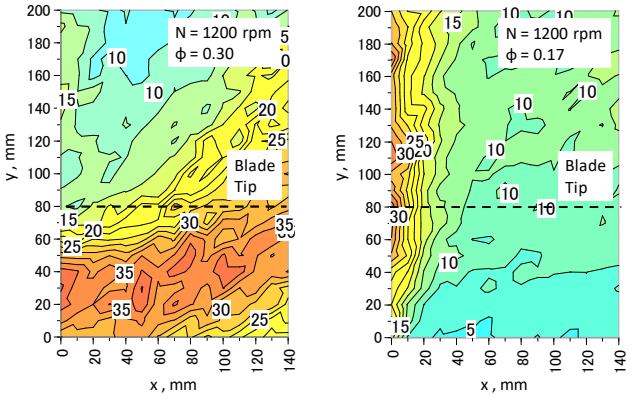

(a) design condition (b) off-design condition

Fig. 8 Distributions of the axial velocity component of the absolute velocity in the meridian plane

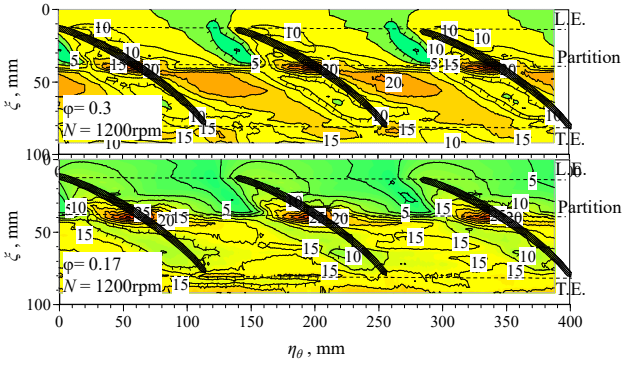

(a) Axial velocity component

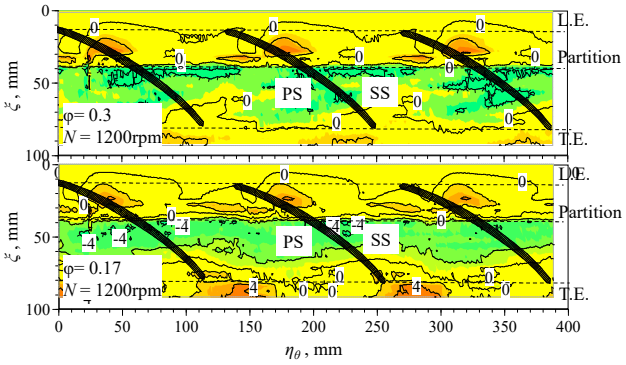

(b) Circumferential velocity component

Fig. 9 Distributions of the absolute velocity in the relative flow field at the blade tip

The spectral distributions of the velocity fluctuations at the blade tip are compared in Fig. 10. The upper figure is the velocity fluctuation variation of the leading edge and the lower one is at the trailing edge. The thick solid line (red) is the variation amount of the off design flow rate, the thin solid line (black) is the design flow rate. These results indicate that the low frequency noise in the off design flow rate is generated by the fluctuation of the low frequency induced by the swirling flow near the leading edge.

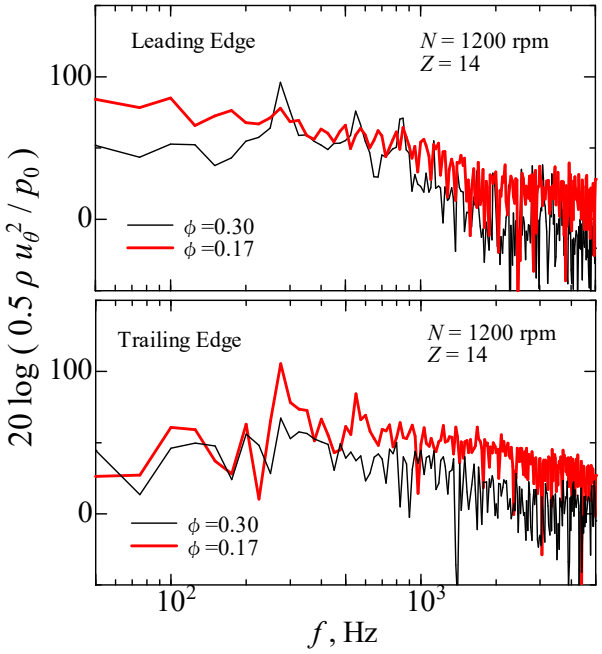

Fig. 10 Spectral distributions of the velocity fluctuations at the blade tip

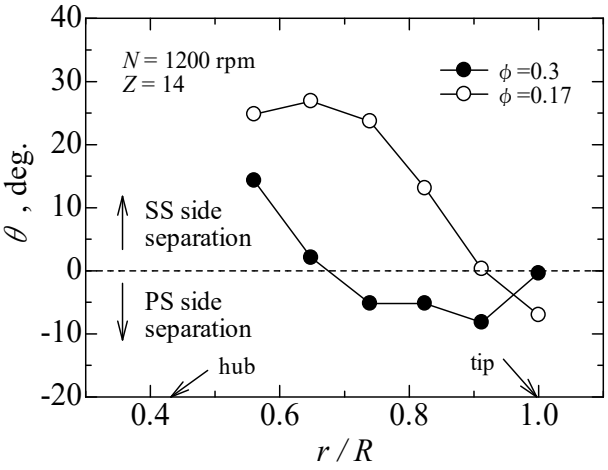

Fig. 11 Distribution of the deviation angle to the span direction in the vicinity of the trailing edge

2.2 Broadband noise of design condition

In Fig. 11, the distribution of the deviation angle to the span direction in the vicinity of the trailing edge is shown. The measurement position is the 5 mm rear side from the trailing edge. The deviation angle is defined as the angle made by the pitch angle γ and the relative flow angle β (see Fig. 12). When the angle is positive, the flow is separated from the suction surface. Whereas, when the angle approaches to 0, the relative flow is

attaches to the blade. ● is the design flow rate; ○ is off design flow rate. This results indicates that the relative flow of the off design flow rate is separated from the suction surface, whereas the relative flow in the design flow rate attaches to the blade.

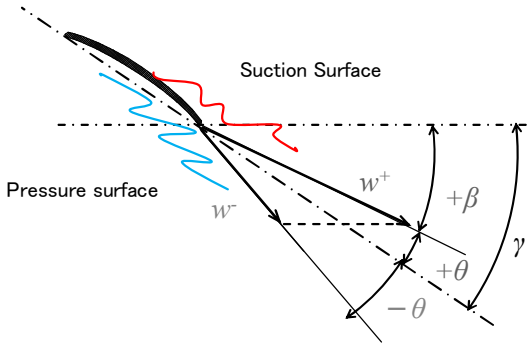

Fig. 12 Definition of the deviation angle

The distributions of the relative flow to the span direction are shown in Fig. 13. Fig. 13 (a) is the relative flow velocity, and Fig. 13 (b) is its velocity fluctuation variation. The velocity and its fluctuation of the off design operation condition are concentrated to the blade tip. This result indicates that the aerodynamic noise source in the off design operation condition is formed at the blade tip side. On the other hand, the relative flow of the design operation condition is widely distributed to the blade span, and its velocity fluctuation becomes large than the off design operation condition.

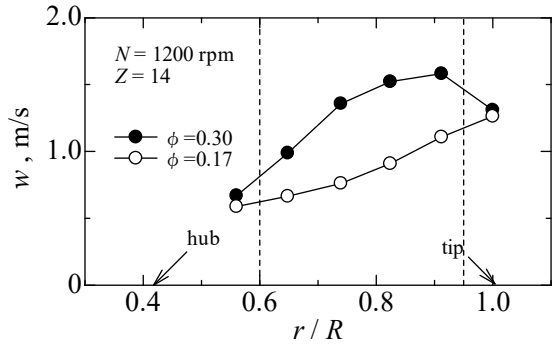

(a) Relative velocity

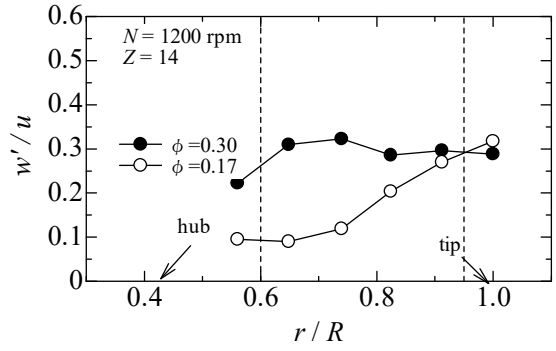

(b) Velocity fluctuation of the relative velocity

Fig. 13 Distributions of the relative flow to the span direction

The pressure fluctuation on the blade surface at the design operation condition calculated by CFD is shown in Fig. 14. The radial position is r / R = 0.74 (R = 230 mm). Fig. 14 (a) is the distribution of the overall pressure fluctuation, and Fig. 14 (b) is the spectral distribution of the sum of the pressure fluctuations of the both blade surface. The pressure fluctuations on the blade surface increase at the leading edge and the trailing edge. This result indicates that the aerodynamic noise source on the blade surface is formed not only at the trailing edge but also at the leading edge. In Fig. 14 (b), the discrete frequency synchronized with the harmonic of the blade passing frequency (BPF) and a discrete frequency of 1560 Hz are formed. The latter discrete frequency may be caused by the vortex shedding frequency of the Karman vortex. The Karman vortex is formed by the interference between the leading edge separation flow and the flow at the trailing edge. This formation of the Karman vortex becomes the factor that of an unstable wave in the blade passage. Furthermore, we can observe the broadband pressure fluctuation around 1000 Hz. This broadband pressure fluctuation is close to the property of broadband noise in the transition frequency generated from the actual propeller fan.

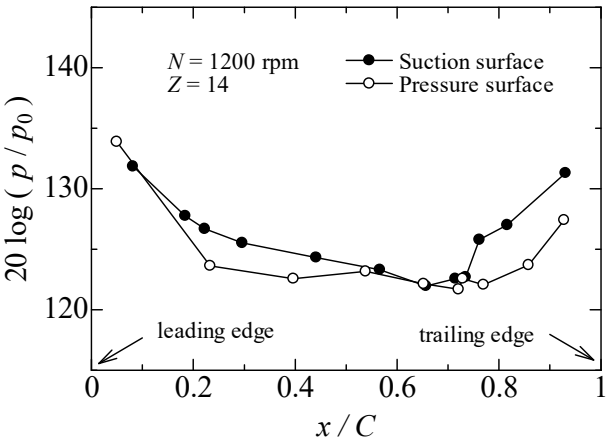

(a) Overall fluctuation on the chord

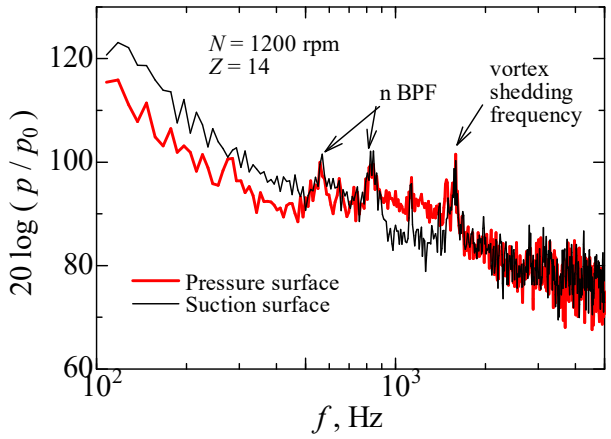

(b) Spectral distribution of the each blade surface

Fig. 14 Pressure fluctuation on the blade surface at the design operation condition

The spectral distribution of pressure fluctuations near the leading edge is shown in Fig. 15. The measurement position is x / C = 0.23 on the pressure surface. In the spectral distribution, a humped pressure fluctuation distribution is formed in the band near 1260 Hz, which is distinguished from the blade passing frequency or the vortex shedding frequency.

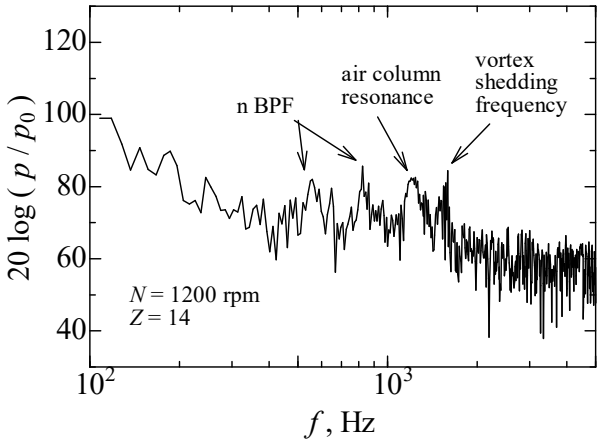

Fig. 15 The spectral distribution of pressure fluctuations near the leading edge (x / C = 0.23)

Let me introduce the air column resonance frequency formed by the blade passage as in the equation (3)

$$f = \frac{n\, a_0}{2\,(\,c + 2\Delta c\,)} \qquad (3)$$

Here,

Δc = 0.6 r, r = 0.5 π D / Z

where, c is the chord length, Δc is the open end correction, and r is the half of the blade pitch. The resonance frequency at each span position estimated by the equation (3) is shown in Table 1. The band of the resonance frequency distributed to the span direction is close to the band of the transition frequency of the fan noise. These results indicate that when the air column resonance occurs in the blade passage at each span position of the propeller fan, the fan generates the broadband noise due to superimpose of the air column resonance noise.

Table 1 Resonance frequency at each span position

r , mm	C, mm	l, mm	Δl, mm	f, Hz
130	72	58.3	17.5	1589
175	92	78.5	23.6	1222
230	101	103.2	31.0	1043
310	122	139.1	41.7	827

3. SUMMARY

(1) The broadband noise of the propeller fan in the off design flow rate became large than that of the design operation condition in the low frequency. The velocity fluctuation having a lower frequency than the blade passing frequency was formed at the leading edge of the blade tip side. The low frequency broadband noise in the off design operation condition has feasibility to generate at the leading edge by adjoined blade interference of the lower frequency than the blade passing frequency. The low frequency broadband noise is even generated in the design operation condition.

(2) The major factor of the fan noise in the design operation condition was the broadband noise in the transition frequency except for the discrete frequency noise due to the mechanical irregularity error of the impeller. The velocity fluctuation of the relative flow at the design operation condition was widely distributed to the span direction of the impeller, and its fluctuation variation was larger than that of the off design operation condition.

(3) From the analysis of CFD, an unstable wave was generated in the blade passage due to the Karman vortex shedding. When the unstable wave resonates with the air column resonance frequency made by the blade passage, the pressure fluctuation having a specific frequency is enhanced in the blade passage. These results indicated that the noise in a specific frequency band increased, even if the fan is operated in the design flow rate, when the air column resonance in the blade passage was superimposed to the span direction.

REFERENCES

(1) Sortor M., On-System Engine Cooling Fan Measurement as a Tool for Optimizing Cooling System Airflow Performance and Noise, SAE International Journal of Materials and Manufacturing, 4 - 1, pp. 1221 – 1230, 2011

(2) Jiang C.-l., Chen J.-p., Chen Z.-j., Tian J., OuYang H., Du Z.-h., Experimental and numerical study on aeroacoustic sound of axial flow fan in room air conditioner, Applied Acoustics, 68 - 4, pp. 458 – 472, 2007

(3) Jang C.-M., Furukawa M., Inoue M., Analysis of vortical flow field in a propeller fan by LDV measurements and LES - Part I: Three-dimensional vortical flow structures, Journal of Fluids Engineering, Transactions of the ASME, 123-4, pp. 748 – 754, 2001

(4) Jang C.-M., Furukawa M., Inoue M., Analysis of vortical flow field in a propeller fan by LDV measurements and LES - Part II: Unsteady nature of vortical flow structures due to tip vortex breakdown, Journal of Fluids Engineering, Transactions of the ASME, 123 – 4, pp. 755 – 761, 2001

(5) FUKANO, T. and JANG, C.-. M, Tip clearance noise of axial flow fans operating at design and off-design condition. *Journal of Sound and Vibration, 275*, pp. 1027-1050, 2004

(6) FUKANO, T., TAKAMATSU, Y. and KODAMA, Y., The effects of tip clearance on the noise of low pressure axial and mixed flow fans. *Journal of Sound and Vibration,* 105 - 2, pp. 291-308. 1986

(7) FUKANO, T., SARUWATARI, H., HAYASHI, H., ISOBE, H. and FUKUHARA, M., Periodic velocity fluctuations in the near wake of a rotating flat-plate blade and their role in the generation of broadband noise. *Journal of Sound and Vibration,* 181-1, pp. 53-70., 1995

(8) ROGER, M. and MOREAU, S., Back-scattering correction and further extensions of Amiet's trailing-edge noise model. Part 1: Theory. *Journal of Sound and Vibration,* 286 - 3, pp. 477-506., 2005

(9) AMIET, R.K., Noise due to turbulent flow past a trailing edge. *Journal of Sound and Vibration,* 47-3, pp. 387-393. 1976